Assessing marine heatwave impacts on the pelagic ecosystem of the San Juan Archipelago

Sarah Hensley

Pelagic Ecosystem Function Apprenticeship

2023

Sarah Hensley
Friday Harbor Laboratories, University of Washington, Friday Harbor, WA 98250
hensley.sarah88@gmail.com | smh68@uw.edu | sarah.hensley@noaa.gov
(360) 870-3923

Keywords: pelagic, ecosystem, marine heatwave, trophic interactions, multi-variate autoregressive model, San Juan Archipelago, Salish Sea

Abstract
In a rapidly changing world, understanding the interactions between the biological and abiotic world is crucial to predict change within our ecosystems and more importantly manage them. With increasing occurrences of marine heatwaves due to climate change, we are provided the unique opportunity to assess how ecosystems respond to intense periods of warming, that produce signals in a pulse-like form. This allows us to gain insight on both how components of our natural marine systems are impacted by warming, as well as how this differs from the more gradual effects, we see with steady increases in temperature due to climate change. In this study, the pelagic ecosystem of the San Juan Archipelago is assessed in relation to its response to the recent 2014-2016 marine heatwave to investigate this. A simplified food web consisting of chlorophyll, pacific sand lance, alcids, gulls, cormorants and pinnipeds is used while chlorophyll, sea surface temperature and photosynthetically active radiation are used as environmental covariates that are tested against the biological components listed above through a multivariate auto-regressive model to assess this question. Time series analyses are also conducted to assess group trends through time, and in relation to pre, during and post heatwave periods. Overall, it was found that all three environmental components (sea surface temperature, photosynthetically active radiation, and chlorophyll) are increasing through time, however sea surface temperature additionally shifted baselines after the heatwave had subsided. When examining the biological components, alcids, gulls and cormorants all have recently made a recovery to pre-heatwave levels after a decline through the heatwave in numbers. In contrast, pinnipeds have been declining continuously throughout time. Several significant interactions were found to be apparent, with sea surface temperature, photosynthetically active radiation and chlorophyll influencing several of the biological groups. Ultimately this indicates that although groups are directly influenced by the environmental covariates tested, which may indicate increased vulnerability to environmental changes due to climate change, biological groups may have the capacity to return to pre-heatwave levels after heatwaves subside. Information as such is critical for further understanding how our ecosystems will change in relation to climate change and also informs that ecosystem responses to marine heatwaves may be different than the more gradual climate change effects, which is important for the management of our systems as a whole.

1. Introduction

Understanding interactions between both the abiotic and biotic components of our world's systems is vital to understanding our ecosystems and their respective dynamics (D'Alpaos, 2009). Furthermore, in the changing climate that earth is currently experiencing, it is even more critical to develop a thorough understanding of these interactions to predict change in our ecological systems and manage commercially, culturally and ecologically important species (Russell et al., 2012). One such facet of climate change that has become much more prominent in our climatic cycles in recent years are marine heatwaves. Although there are many varying definitions of marine heatwaves, they can be generally defined as periods in time where temperatures are consistently above a given threshold (Oliver et al. 2020). These events have not only been increasing in frequency through time, but also have been increasing in intensity as well (Oliver et al. 2018). In addition, conditions post-heatwave have been seen to remain different than pre-heatwave years, thus suggesting a shifted baseline of the given condition being assessed, producing a potentially permanent change to the abiotic environment that ecosystems inhabit. Given the direct influence that marine heatwaves have on the physical and chemical processes, the implications for the biological components of the system that rely on the physical and chemical composition of their environments for survival can be significant (Frölicher et al. 2018). A unique feature however of marine heatwaves is the pulse like signal that these extreme temperatures present themselves in (Oliver et al. 2018). Given the short-term, high-intensity changes to the environment that this results in, marine heatwaves also present unique opportunities to study changes and responses within a system in intense warming periods representative of climate change. The information that this presents is therefore very valuable for managers, as it enables us to understand population responses as well as thresholds for resiliency within our systems, which can better inform decisions related to mitigating climate change impacts.

To assess this wealth of information, an intensive study of interactions is required to understand how marine heatwave signals propagate through our systems. One such tool to do so are multivariate autoregressive (MAR) models, which enable us to assess interactions between both the biotic and abiotic features of our system as well as the interactions of the biotic components with themselves (Hampton et al., 2013; Ives et al., 2003). Within this model framework, we can compare multiple unlike variables through time, allowing us a time series approach to address questions regarding change over time as with climate change impacts on ecosystems (Mac Nally et al., 2010; Hampton et al., 2013). The parameter outputs produced through this model therefore give us an understanding of how these components influence one another, which allows us insight on which groups within an ecosystem may be most vulnerable to perturbations, as well as what those responses may be. Given the insight that this allows us into ecosystem response, the MAR model has the potential to provide key supplemental information to help inform management decisions.

As a case study of the impacts of marine heatwaves, the pelagic ecosystem of the San Juan Archipelago was selected as a focal system to better understand ecosystem responses to these pulse-like intense temperatures, given the recent occurrence of heatwaves in the region. Located in the estuarian waters between Washington State and Canada (*Figure 1*), this system presents both a diverse range of biota with high rates of productivity, as well as profound oceanographic

features such as upwelling/downwelling phenomena and both fresh and saltwater inputs (Royer 1998; Mundy et al. 2010). In recent years, heat waves have started to increase in frequency within the region, with one major heatwave occurring at the end of 2014 and propagating through 2016. Temperatures throughout this time were seen to be up to 2.3°C higher than normal and resulted in changes within various lower trophic groups such as phytoplankton and zooplankton (Khangaonkar et al., 2021). As noted, given that shifts within lower trophic groups were seen within this ecosystem, we can draw the conclusion that changes within the system were occurring.

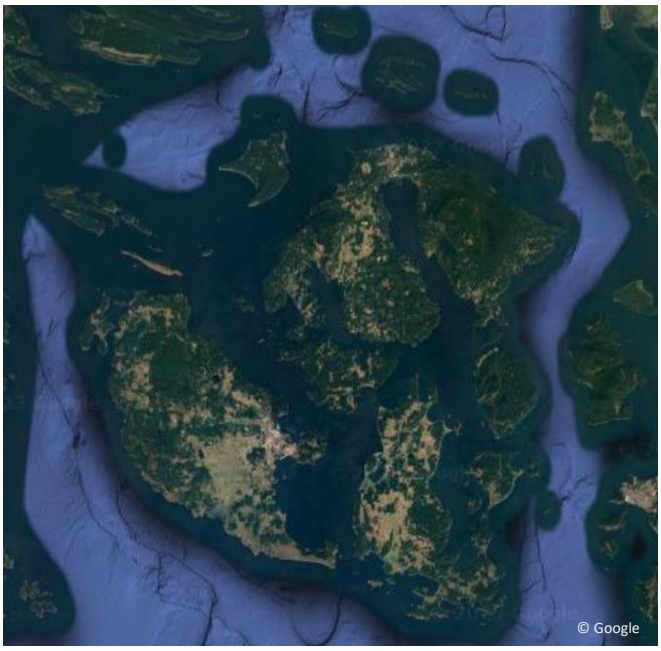

Figure 1. Depicted above is the San Juan Archipelago. Green objects indicate land, dark blue objects indicate inter-island waters and light blue indicates the broader ocean masses that flow between the United States and Canada.

To determine what the specific impacts of this heatwave were throughout the entire ecosystem, and more specifically whether the signal produced by the 2014-2016 marine heatwave resonated for sustained periods of time post-heatwave, this study uses a modeling approach similar to that of which was discussed above to allow for a quantitative assessment of how the San Juan Archipelago pelagic ecosystem has been changing over time, in relation to the increased frequency of marine heatwaves. Here we focus on a subsection of the ecosystem to focus on key documented players within the ecosystem, incorporating oceanographic, fish and marine mammal and bird indices over a thirteen-year time series starting in 2010 and ending in 2022. This incorporates periods prior to the heatwave from 2010-2013, periods during the heatwave from 2014-2016, and periods after the heatwave from 2017-2022. Through these analyses, our study seeks to inform on the signal of the marine heatwave throughout the ecosystem of this region, and which groups were most directly impacted. Additionally, this study seeks to present supplemental information of marine heatwave impacts generally across ecosystems, and the incorporation of this information into management and recovery plans for ecosystems in response to climate change.

2. Materials and Methods

2.1 Model Variables

Selection and assimilation of the data that are used as inputs into the MAR model for parameter estimates were dictated by availability of data and robustness. In addition, the selected factors for this study were based on their relevance to the ecosystem as well as life history, and influence on biological processes. A simplified food web was constructed to incorporate abiotic components as well as primary, secondary and tertiary trophic groups to allow for a holistic yet manageable overview of how the pelagic ecosystem would be influenced in different ways. For oceanographic indices, sea surface temperature (SST °C), photosynthetically active radiation (PAR einstein m^{-2} day^{-1}), and chlorophyll (mg/m^3) were used. SST was selected for its influence on both the lifecycle of primary producer groups as well as the metabolism of secondary and tertiary trophic groups. PAR was selected for its relevance to primary producer groups while chlorophyll was selected as a proxy for phytoplankton abundance. SST was extrapolated from the Hadley Centre Sea Ice and Sea Surface Temperature (HadISST) dataset, which combines satellite and in-situ SST measurements to construct monthly SST outputs, located within the National Oceanic and Atmospheric Administration's (NOAA) Environmental Research Division Data Access Program (ERDDAP) database. Both PAR and chlorophyll were extrapolated directly from the National Aeronautics and Space Administration (NASA) Aqua Moderate Resolution Imaging Spectroradiometer (MODIS) satellite output and were also accessed through the NOAA ERDDAP database. For fish indices, Pacific Sand Lance (*Ammodytes personatus*) were selected as the main study species to fulfill the forage fish trophic level, given their biological importance to the area as well as abundance (Zamon 2017). The indices used were fish condition (K)—used as a measure of fish energetics—and CPUE, measured via Van Veen sampling methods as a proxy for fish abundance. Sampling of these fish occurred in the San Juan Channel where a major sand wave field is present within the San Juan Archipelago which has been deemed preferred habitat of this species within this region (Greene et al. 2010). For marine mammal and bird indices, density was used as a measure of observed abundance. For marine birds, alcid (*Alcidae*), cormorant (*Phalacrocoracidae*), and gull (*Laridae*) groups were assessed to incorporate different life histories and foraging strategies into the food web structure of our model. Alcids and cormorants represent diving birds, whereas gulls represent surface feeders, thus presenting two potential different impact points of marine heatwaves. Additionally, for size comparison, alcids and cormorants were both included to develop an understanding if different size classes of marine birds are impacted differently. For surface feeder birds, there were no other prominent groups with sufficient data to accurately compare the impact of the marine heatwave in comparison to gulls. For marine mammals, pinnipeds (*Pinnipedia*) were selected as this is a key group of marine mammal species to the area and additionally have plentiful data to allow for analysis.

2.2 Sampling methods

2.2.a Pacific Sand Lance Sampling

For the index for Pacific Sand Lance, sample data from the San Juan Channel wave field sampling site was selected for this study (*Figure 2A*), ranging from a time frame of the 25th of

September to the 15th of November for the purposes of standardization. The sampling site within San Juan Channel (SJC) is defined by a major sand-wave field extending roughly 2 kilometers with deep-water features ranging up to 80m (Greene et al. 2010). Van Veen sampling was conducted here once a week and was deployed from the R/V 'Centennial', R/V 'Auklet' and R/V 'Kittiwake'. The Van Veen mechanism emulates a large scoop, which is deployed off the back of the respective boat via a pulley system, which is lowered steadily until it reaches the ocean bottom. Upon hitting the bottom, the Van Veen snaps shut and ideally scoops the sediment below. Given that Pacific Sand Lance occupy sediment areas as mentioned above (Greene et al. 2010), this allows for the capture of the specimens. A maximum volume of 0.026 m^3 is captured upon closing of the Van Veen across a 0.12 m^2 surface area. Across the entire time series, 271 Van Veen grabs successfully closed. All fish sampled in incomplete grabs that did not fully close were excluded for the purpose of this study. Following capture, the fish were then processed back at the University of Washington Friday Harbor Laboratory Station according to the University of Washington Institutional Animal Care and Use (IACUC) Protocol 4238-03. A lethal dose of anesthetic tricaine methanesulfonate (MS-222) was administered prior to measuring the fork length (mm) and total length (mm) of the fish, as well as measuring their wet weight (g). In the years 2010-2012, fork length was strictly recorded, for which a linear regression was run between fork length and total length to convert fork length to total length for these years, for the purposes of making condition assessments. This decision was made given that in the years 2021-2022, total length was the only length measurement recorded.

2.2.b. Marine Bird and Mammal Sampling

Marine bird and mammal sampling occurred along a consistent transect covering an area of 8.4 km^2 within the San Juan Channel, which was divided across six zones based on geographic features of the transect. These were conducted on the R/V 'Centennial' and R/V 'Kittiwake', roughly six times each year. Sampling occurred from both the starboard and port side on the top deck of the respective research vessels, depending on the year of sampling. A minimum of two observers were present each time and used binoculars to conduct their surveys. Survey calls were made once every minute, and each individual bird and mammal were only counted once and recorded. A range of 200m from the boat was also used as a standard measuring metric for counting animals. Species, number of individuals, and time were recorded. Species spotted on land were also excluded for the purposes of this study. The raw observed abundances measured were then transformed into density (individual/km^2).

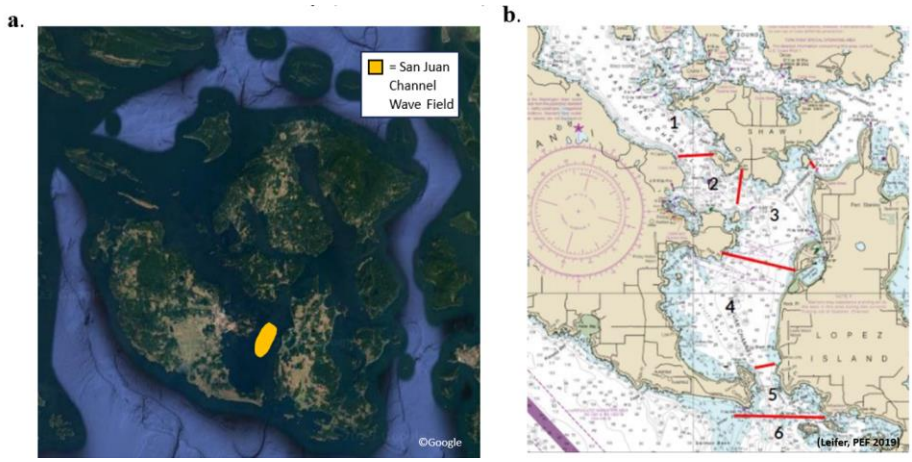

Figure 2. Depicted above is an outline of where sampling for the biological parameters of pacific sand lance and marine mammal and bird sampling took place. Figure 2A depicts the San Juan Channel Wave Field in orange, this being these location from which our sample fish came from. Figure 2B depicts the different zones within the transect that was run for marine mammal and bird sampling.

2.3 Data Processing

To assimilate the data into the models for this study, a series of rigorous data filtering methods were used. The methods for each group of indices are outlined below.

2.3.a. Oceanographic Indices

For oceanographic indices, the raw data outputs of SST, PAR and chlorophyll were converted into monthly and annual averages across the time series. This was done in R Studio using the summarise(mean()) function.

2.3.b. Fish Indices

For fish indices, data was assimilated across the years 2010-2022. For condition, data was assimilated across the time series of all available records of fish morphometrics from every year with notes on the date of sampling, sampling method (Van Veen), location of sampling (SJC), fork length (mm), total length (mm), calculated total length (mm), wet weight (g), and condition factor (K). Condition factor (K) was calculated using the below formula (Bagenal & Ricker 1978):

$$K = m \times 10^{7} \times l^{-3}$$

where m is representative of mass (in g) and l is representative of total length (in mm). All fish that were used for tank experiments were removed for the purposes of keeping our samples representative of wild fish within the ecosystem. For the calculation of CPUE, data from Van Veen sampling events were assimilated with the inclusion of sampling date, location, total number of grab attempts, total number of successful grabs, total number of successful grabs at SJC, raw number of fish caught per sampling event, CPUE for the total cruise time, and CPUE for strictly the SJC sampling events. Note that the year 2022 was dropped in for CPUE due to errors in data entry. For the purposes of comparison across years, all data was filtered for SJC sampling events given that this was the main consistent sampling location across years. Monthly

and annual averages were then again calculated using the summarise(mean()) function in R Studio. CPUE for the Van Veen sampling events was calculated via the following equation:

$$CPUE = total\ \#\ of\ fish\ individuals/grab$$

2.3.c. Marine Mammal and Bird Indices

Data on marine mammal and bird observation events were assimilated across the 2010-2022 time series. The information included in this dataset were year, date of sampling, species code, common name, group, density, and effort/km^2. Monthly and annual averages were then calculated using the summarise(mean()) function in R Studio, based on each respective group.

2.4 Statistical Analyses

2.4.a Preliminary Statistics

All data analyses were performed using R 4.2.3 in R Studio. The initial analysis conducted included producing linear regressions and box plots of all variables to get an understanding of the spread of data and inherent trends. Furthermore, shifting baseline plots were generated by averaging means of the given variable across the three different marine heatwave regimes (pre-heatwave: 2010-2013, during heatwave: 2014-2016, post-heatwave: 2017-2022). For marine mammals and birds only, a shifting trends plot was generated rather than a shifting baselines plot, where trends within the different heatwave regimes outlined above were assessed separately to encapsulate degree of recovery by the system in more recent years to account for the influence that a lag time in population recovery might have. These trends were also assessed via linear regressions. Additionally, correlation plots using the PerformanceAnalystics package were generated to understand inherent interactions within the oceanographic indices and biological components, prior to comparing them to the rest of the indices in the system. After completing these analyses, an ANOVA test and Tukey-test was performed on the variables where shifting baselines were found to be potential phenomena. The outputs from these tests then allowed us to determine whether post-heatwave conditions were significantly different than pre-heatwave conditions, indicating a shifted baseline.

2.4.b MAR Model

Following this, all variables were inputted into the same datafile to be filtered through the R model. The structure of the MAR model was based on the following formula:

$$x_t = Bx_{t-1} + a + Cu_{t-1} + w_t$$

with x_t representing the abundance in the current time step, x_{t-1}representing the abundance in the previous time step, *B* representing the effect of a given groups density on the growth rate of another group (density dependence), a being the intrinsic rate of increase for a species, *C* being the effect of the covariate being tested on the other group, u_{t-1}being the covariate value of the previous time step, and w_t being the process error inherent with estimations of the model (Hampton et al. 2013). A matrix format for relationships between groups is inherently tested in this model, and for the purposes of this study is formatted in the following way:

$$\begin{bmatrix} P_{t+1} \\ C_{t+1} \\ S_{t+1} \\ CF_{t+1} \\ V_{t+1} \\ PI_{t+1} \\ A_{t+1} \\ G_{t+1} \\ CO_{t+1} \end{bmatrix}_{t+1} = \begin{bmatrix} b_{PP} & b_{PC} & b_{PS} & b_{PCF} & b_{PV} & b_{PPI} & b_{PA} & b_{PG} & b_{PCO} \\ b_{CP} & b_{CC} & b_{CS} & b_{CCF} & b_{CV} & b_{CPI} & b_{CA} & b_{CG} & b_{CCO} \\ b_{SP} & b_{SC} & b_{SS} & b_{SCF} & b_{SV} & b_{SPI} & b_{SA} & b_{SG} & b_{SCO} \\ b_{CFP} & b_{CFC} & b_{CFS} & b_{CFCF} & b_{CFV} & b_{CFPI} & b_{CFA} & b_{CFG} & b_{CFCO} \\ b_{VP} & b_{VC} & b_{VS} & b_{VCF} & b_{VV} & b_{VPI} & b_{VA} & b_{VG} & b_{VCO} \\ b_{PIP} & b_{PIC} & b_{PIS} & b_{PICF} & b_{PIV} & b_{PIPI} & b_{PIA} & b_{PIG} & b_{PICO} \\ b_{AP} & b_{AC} & b_{AS} & b_{ACF} & b_{AV} & b_{API} & b_{AA} & b_{AG} & b_{ACO} \\ b_{GP} & b_{GC} & b_{GS} & b_{GCF} & b_{GV} & b_{GPI} & b_{GA} & b_{GG} & b_{GCO} \\ b_{COP} & b_{COC} & b_{COS} & b_{COCF} & b_{COV} & b_{COPI} & b_{COA} & b_{COG} & b_{COCO} \end{bmatrix}_{t} * \begin{bmatrix} P_t \\ C_t \\ S_t \\ CF_t \\ V_t \\ PI_t \\ A_t \\ G_t \\ CO_t \end{bmatrix}_{t}$$

where P represents PAR, C represents Chlorophyll, S represents SST, CF represents pacific sand lance condition factor, V represents Van Veen CPUE (fish abundance), PI represents pinniped density, A represents alcid density, G represents gull density, and CO represents cormorant density. The outputs of this model are outputs representative of the relationship between the two groups being tested for interaction. Positive parameter outputs indicate a positive relationship between the two groups, while a negative parameter output indicates a negative relationship between the two groups. Confidence intervals are added to these parameter outputs to account for process error inherent in the model. Given the 13-year time series constraint within our dataset, the Broyden-Fletcher-Goldfarb-Shanno (BFGS) algorithm method was used for the computation of the MAR model.

3. Results

The analysis of this study focused on three trophic levels encompassing chlorophyll, pacific sand lance (forage fish), pinnipeds and gulls, cormorants and alcids (marine mammals and birds) as mentioned above. After data synthesis was completed, a total time series of 13 years was available for the purposes of this study, spanning 2010-2022.

3.a. Time Series Analyses

3.a.i. Sea Surface Temperature

Sea surface temperature was examined in three different ways. First, annual averages for each year within our time series were calculated to see what the average trend throughout our time period was (*Figure 3A*). The results indicated a significant positive trend in sea surface temperature through time (*p-value = 0.034*). This was then broken down by months, to highlight annual trends across the months of interest to this study: September through November (*Figure 3C*). It was found that there was a slight positive trend throughout our time series in each of the above three months, however the significance of this positive trend decreased through the season (*September p-value: 0.120, October p-value: 0.376, November p-value: 0.577*). Thirdly, an examination of mean temperatures prior to, during and after the heatwave was conducted to determine if a shifted baseline had occurred. For sea surface temperature, mean temperatures prior to the heatwave were 10.5 °C, 11.6 °C during the heatwave and 11.1 °C after the heatwave (*Figure 3B)*. The Tukey-test results (*Table 1*) revealed that there was a significant difference across all three groups, and most importantly indicated that there was a significant difference between pre-heatwave and post-heatwave temperatures, indicating that a shifting baseline of sea surface temperature had occurred post-heatwave (*p-value = 0.017*).

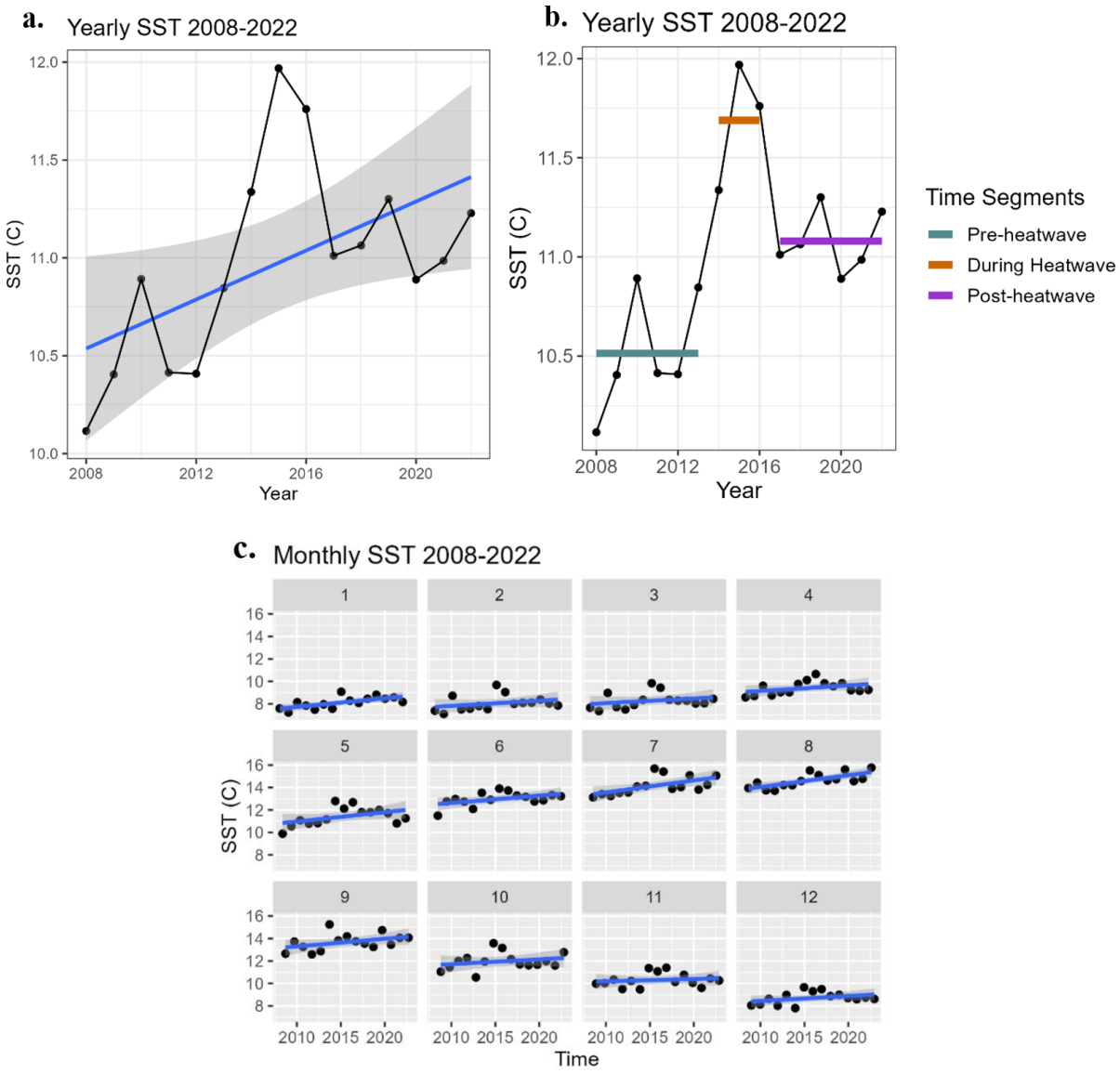

Figure 3. Depicted above are annual averages of sea surface temperature. Figure 3A displays annual averages of sea surface temperature through time (black line), with year on the x-axis and sea surface temperature in Celsius on the y-axis. A linear regression is depicted in blue, with confidence intervals depicted in the shaded grey region. With this, a positive trend is depicted through time. Figure 3B displays the same annual average data (black line) with year on the x-axis and sea surface temperature in Celsius on the y-axis. The blue, orange and purple lines depict the average sea surface temperatures within the heatwave regimes indicated under "Time Segments". This plot displays a shifted baseline for temperature after the heatwave rescinded, as post-heatwave temperatures are significantly greater than pre-heatwave temperatures (*p-value = 0.017*). Figure 3C displays averages for each month of every year, to generate an annual breakdown of average temperatures in the given month across time, with year across the x-axis, sea surface temperature in Celsius on the y-axis. The bands across the top of each plot within the figure indicate the month for which the annual averages represent, while the black points indicate

these annual averages, and the blue line indicates the general trend as determined by a linear regression.

Table 1. Depicted below are the results of the Tukey Honest Significant Difference test when average temperatures across the different marine heatwave regimes were compared. In the left column, the comparison tested by the test is outlined while the right column indicates their respective p-values. “Post” indicates post-heatwave, “HW” indicates heatwave, and “Pre” indicates pre-heatwave. “Post-HW” therefore compares post-heatwave temperatures to heatwave temperatures. * indicates that the p-value was found to be significant.

Variables Tested	p-value
Post-HW	0.021*
Pre-HW	0.0000989*
Pre-Post	0.017*

3.a.ii. Photosynthetically Active Radiation

Photosynthetically Active Radiation (PAR) was also examined in three different ways. Annual averages were first calculated to determine the average trend of PAR throughout our entire time series, for which a positive trend was detected (*Figure 4A, p-value = 0.407*). These annual averages were also broken down by month to again allow us to highlight the annual trends within our study period (*Figure 4C*). Here, no trend was detected for the months of September and November (*September p-value = 0.943, November p-value = 0.985*), however a positive trend was detected for the month of October (*October p-value = 0.519*). Thirdly, mean PAR values broken down by pre, during and post heatwave regimes were measured to examine whether a shifted baseline had also occurred. Mean PAR values were found to be 27.6 einstein m^{-2} day^{-1} pre-heatwave, 30.9 einstein m^{-2} day^{-1} during the heatwave, and 29.0 einstein m^{-2} day^{-1} post-heatwave. The Tukey-test results (*Figure 2*) revealed that there was a significant difference across one of the three groups, being pre-heatwave versus during heatwave PAR levels (*p-value = 0.005*). Although PAR values did not return to pre-heatwave levels after the heatwave subsided, the difference in average temperatures between pre and post heatwave were not found to be significant (*p-value = 0.*128). Given this, it was determined that there was not a significant shift in baselines in PAR after the heatwave. It is important to note however that post-heatwave temperatures were not found to be significantly different than during heatwave PAR levels, and therefore although a significant shifted baseline cannot be determined for PAR, PAR values more closely mirrored heatwave PAR levels than pre-heatwave PAR levels.

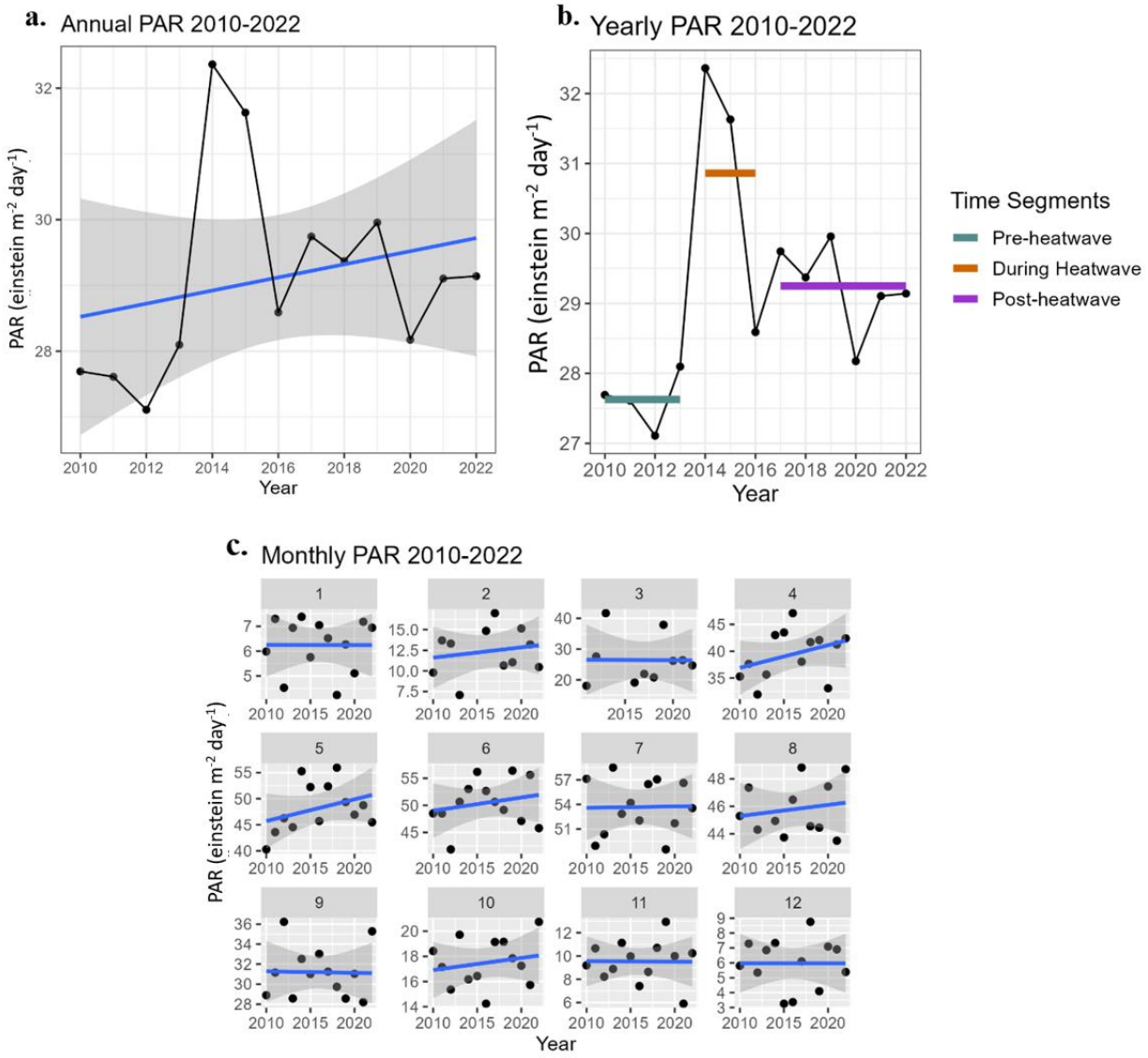

Figure 4. Depicted above are annual averages of photosynthetically active radiation (PAR). Figure 4A displays annual averages of PAR through time (black line), with year on the x-axis and PAR in einstein m^{-2} day^{-1} on the y-axis. A linear regression is depicted in blue, with confidence intervals depicted in the shaded grey region. With this, a positive trend is depicted through time. Figure 4B displays the same annual average data (black line) with year on the x-axis and PAR in einstein m^{-2} day^{-1} on the y-axis. The blue, orange and purple lines depict the average PAR within the heatwave regimes indicated under "Time Segments". This plot displays a near significant shifted baseline for PAR after the heatwave rescinded, as post-heatwave PAR levels are close to being significantly greater than pre-heatwave PAR levels but are not truly significant (*p-value = 0.128*). Figure 4C displays averages for each month of every year, to generate an annual breakdown of average PAR in the given month across time, with year across the x-axis, PAR in einstein m^{-2} day^{-1} on the y-axis. The bands across the top of each plot within the figure indicate the month for which the annual averages represent, while the black points indicate these annual averages, and the blue line indicates the general trend as determined by a linear regression.

Table 2. Depicted below are the results of the Tukey Honest Significant Difference test when average PAR across the different marine heatwave regimes were compared. In the left column, the comparison tested by the test is outlined while the right column indicates their respective p-values. "Post" indicates post-heatwave, "HW" indicates heatwave, and "Pre" indicates pre-heatwave. "Post-HW" therefore compares post-heatwave temperatures to heatwave temperatures. * indicates a significant p-value.

Variables Tested	p-value
Post-HW	0.115
Pre-HW	0.005*
Pre-Post	0.128

3.a.iii. Chlorophyll

Lastly for environmental covariates, chlorophyll was also examined in three different ways. Annual averages were calculated first to assess the general trend of chlorophyll values throughout the entire time series, for which a positive trend was detected, although less significant than both trends in SST and PAR (*Figure 5A, p-value = 0.287*). These averages were then again broken down by month to focus on the months within our study (*Figure 5C*). When doing so, chlorophyll levels were found to follow a decreasing trend across all three study months through time (*September p-value = 0.512, October p-value = 0.328, November p-value = 0.164*). The third analysis conducted was again an assessment of whether a shifted baseline phenomena had occurred (*Figure 5B*). Mean chlorophyll levels indicated 7.2 mg/m^3 pre-heatwave, 7.6 mg/m^3 during the heatwave, and 7.3 mg/m^3 post-heatwave. The Tukey-test results (*Table 3*) revealed that there was no significant difference between any of the heat wave regimes, and more specifically no difference in pre-heatwave to post-heatwave chlorophyll levels (*p-value = 0.604*) and therefore it was determined that no shifting baseline occurred.

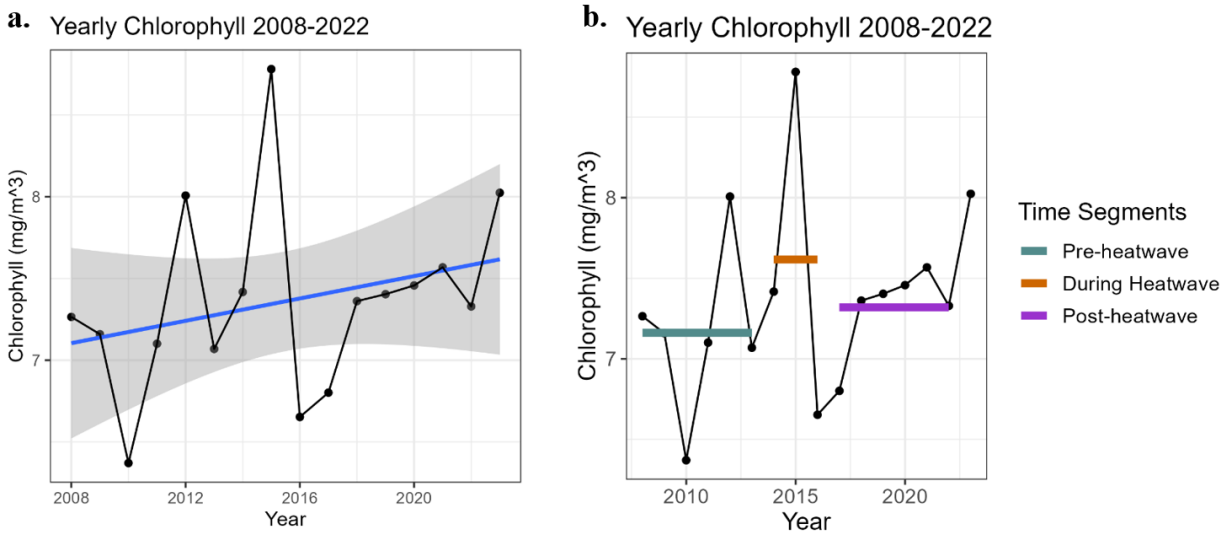

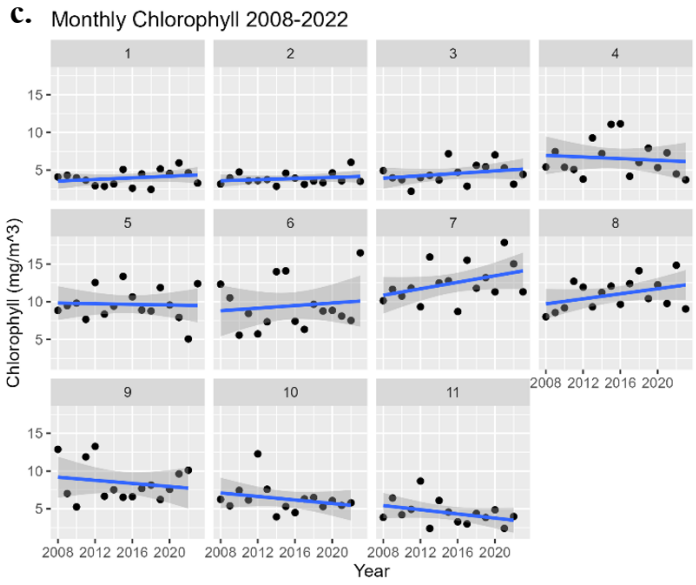

Figure 5. Depicted above are annual averages of chlorophyll. Figure 5A displays annual averages of chlorophyll through time (black line), with year on the x-axis and chlorophyll in mg/m^3 on the y-axis. A linear regression is depicted in blue, with confidence intervals depicted in the shaded grey region. With this, a positive trend is depicted through time. Figure 5B displays the same annual average data (black line) with year on the x-axis and chlorophyll in mg/m^3 on the y-axis. The blue, orange and purple lines depict the average chlorophyll within the heatwave regimes indicated under "Time Segments". No significant shifted baseline was detected for chlorophyll (*p-value = 0.604*). Figure 5C displays averages for each month of every year, to generate an annual breakdown of average chlorophyll in the given month across time, with year across the x-axis, chlorophyll in mg/m^3 on the y-axis. The bands across the top of each plot within the figure indicate the month for which the annual averages represent, while the black points indicate these annual averages, and the blue line indicates the general trend as determined by a linear regression.

Table 3. Depicted below are the results of the Tukey Honest Significant Difference test when average chlorophyll across the different marine heatwave regimes were compared. In the left column, the comparison tested by the test is outlined while the right column indicates their respective p-values. "Post" indicates post-heatwave, "HW" indicates heatwave, and "Pre" indicates pre-heatwave. "Post-HW" therefore compares post-heatwave temperatures to heatwave temperatures.

Variables Tested	p-value
Post-HW	0.956
Pre-HW	0.820
Pre-Post	0.604

3.a.iv. Pacific Sand Lance Condition

Beginning with the biological parameters tested in this study, Pacific Sand Lance condition was calculated and examined through the 2010-2022 time period. To assess the average condition through time and incorporate the variability inherent in biological parameters such as condition factor (K), a boxplot was used to display condition of pacific sand lance through time (*Figure 6A*). Additionally, an analysis of whether condition factor had shifted baselines was also conducted via a similar calculation of means by heatwave regime as noted above (*Figure 6B*). It was found that pre-heatwave condition factor levels were around 29.4, and post-heatwave condition factor levels were around 29.8 while during the heatwave condition factor levels were around 24.9. A dip in condition factor was therefore noted nearly immediately after the onset of the marine heatwave in 2014, however the fish condition rapidly increased again to reach pre-heatwave levels by the end of the heatwave. The Tukey-test results (*Table 4*) revealed that pre-heatwave fish condition levels as compared to post-heatwave fish condition levels were not statistically different (*p-value = 0.914*), supporting this conclusion. It is important to note that pre-heatwave condition factor levels were still reached and maintained by pacific sand lance, despite the shifted baseline for sea surface temperature that we noted above.

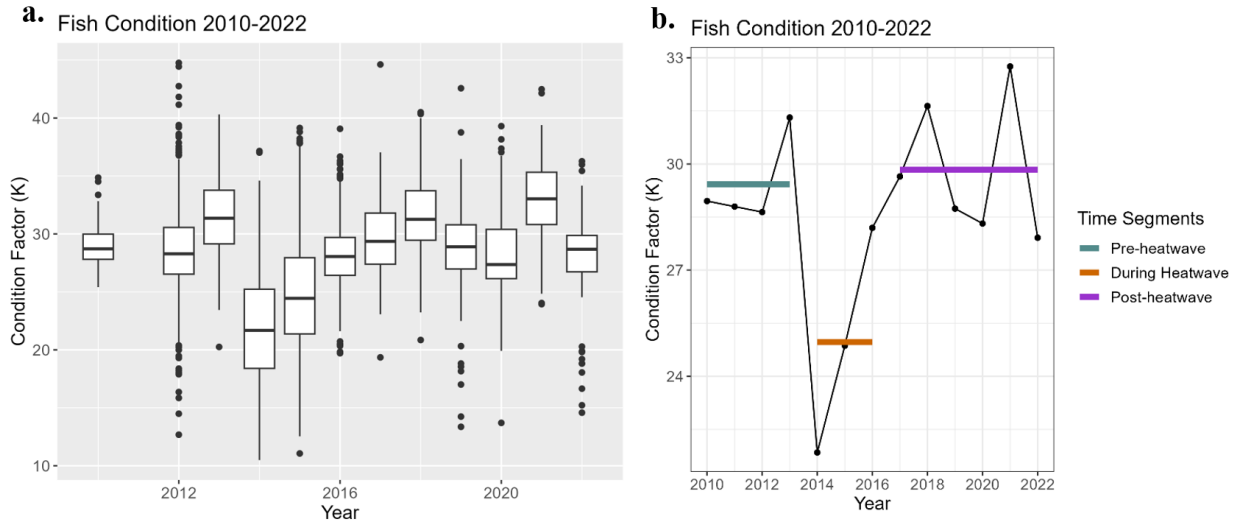

Figure 6. Depicted above is annual fish condition with year plotted on the x-axis and condition factor (K) plotted on the y-axis for both figures. Figure 6A indicates fish condition in a box plot format, with medians of fish condition annually being depicted by the central line within the box plot. Figure 6B indicates fish condition on an annual scale (black line), while the means based on heat wave regimes outlined under "Time Segments" are depicted on top of the annual average fish condition values in color.

Table 4. Depicted below are the results of the Tukey Honest Significant Difference test when average fish condition (K) across the different marine heatwave regimes were compared. In the left column, the comparison tested by the test is outlined while the right column indicates their respective p-values. "Post" indicates post-heatwave, "HW" indicates heatwave, and "Pre" indicates pre-heatwave. "Post-HW" therefore compares post-heatwave temperatures to heatwave temperatures.

Variables Tested	p-value
Post-HW	0.055
Pre-HW	0.128
Pre-Post	0.914

3.a.v. Pacific Sand Lance Abundance

Similar to the analyses done for pacific sand lance condition, a boxplot and shifted baseline plot were generated in order to assess pacific sand lance abundance over time as well as whether mean abundances had shifted throughout the different heatwave regimes (*Figure 7A*). Fish abundance as displayed in the box plot remains on a relatively consistent boom and bust cycle, with an increasing trend through the marine heatwave in 2014-2016. When examining mean abundance levels across the heatwave regimes, a mean of 11.8 fish/grab were noted prior to the heatwave, 10.5 fish/grab during the heatwave and 10.2 fish/grab after the heatwave (*Figure 7B*). The results of the Tukey-test (*Table 5*) indicated a non-significant difference between pre-heatwave and post-heatwave abundance, allowing us to conclude fish abundance likely did not shift baselines. It is important to note however the peak fish abundance that was witnessed during the heatwave.

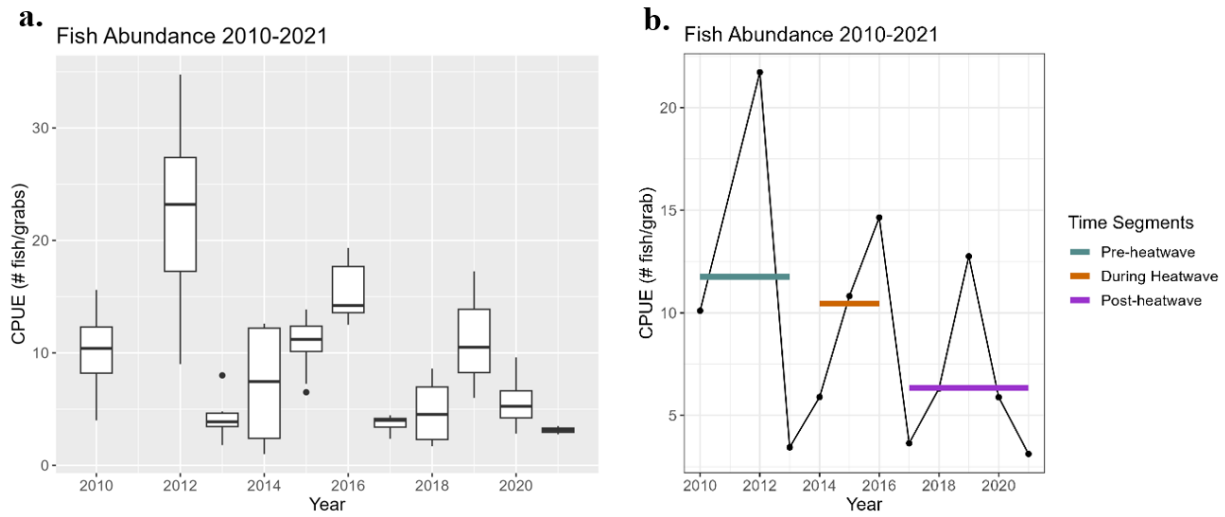

Figure 7. Depicted above is annual fish abundance with year plotted on the x-axis and CPUE (#fish/grab) plotted on the y-axis for both figures. Figure 7A indicates fish abundance in a box plot format, with medians of fish abundance annually being depicted by the central line within the box plot. Figure 7B indicates fish abundance on an annual scale (black line), while the means based on heat wave regimes outlined under "Time Segments" are depicted on top of the annual average fish abundance values in color.

Table 5. Depicted below are the results of the Tukey Honest Significant Difference test when average fish abundance (CPUE) across the different marine heatwave regimes were compared. In the left column, the comparison tested by the test is outlined while the right column indicates their respective p-values. "Post" indicates post-heatwave, "HW" indicates heatwave, and "Pre" indicates pre-heatwave. "Post-HW" therefore compares post-heatwave temperatures to heatwave temperatures.

Variables Tested	p-value
Post-HW	0.968
Pre-HW	0.953
Pre-Post	0.847

3.a.vi. Marine mammal and bird observed abundance

For the assessment of pinnipeds as well as gulls, alcids and cormorants through time, annual observed abundance was plotted on an annual time scale on a linear regression model to perceive general trends through time (*Figure 8A*), while trends by marine heatwave regimes were also assessed to determine whether shifted baselines had occurred (*Figure 8B*). For pinnipeds, a consistent negative linear trend was detected throughout the time series (*p-value = 0.000186*). In contrast, a general negative trend was detected for alcids (*p-value = 0.764*) and gulls (*p-value = 0.312*) while a slight positive trend was detected for cormorants (*p-value = 0.128*). However, when assessing this data from a marine heatwave regime perspective, it is apparent that the linear declining trends for alcids and gulls smooth over a recent increase that these groups have had since the subsiding of the 2014-2016 marine heatwave. Given this, we were able to conclude that alcids, gulls and cormorants all declined in response to the heatwave, however their populations have been slowly rebounding. In contrast for pinnipeds, the strong linear negative trend in their decline indicates no return to previous population numbers.

a.

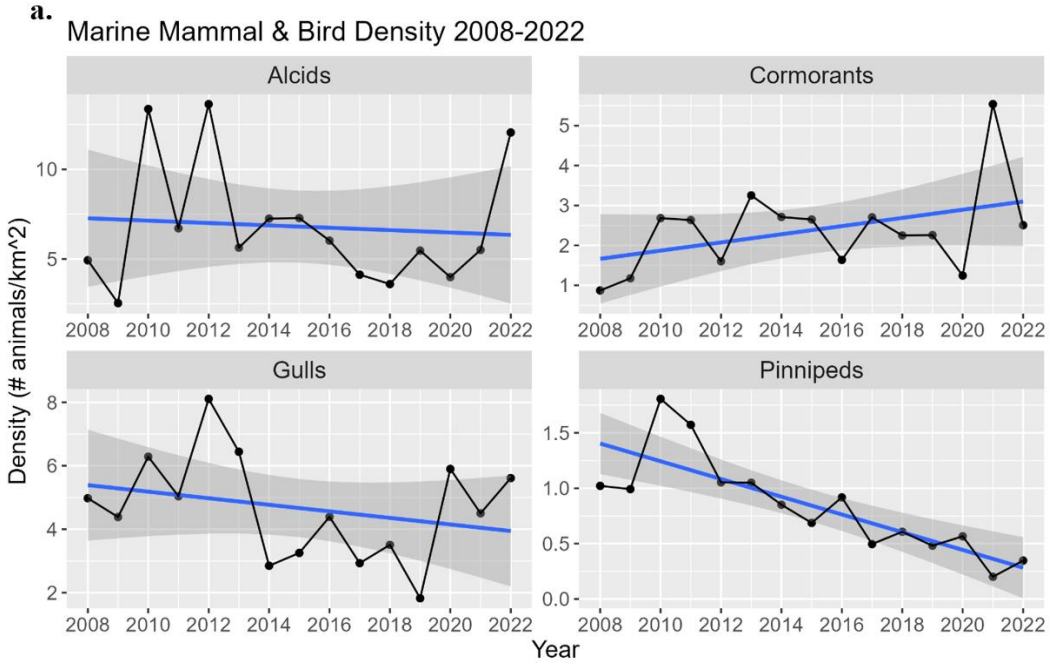

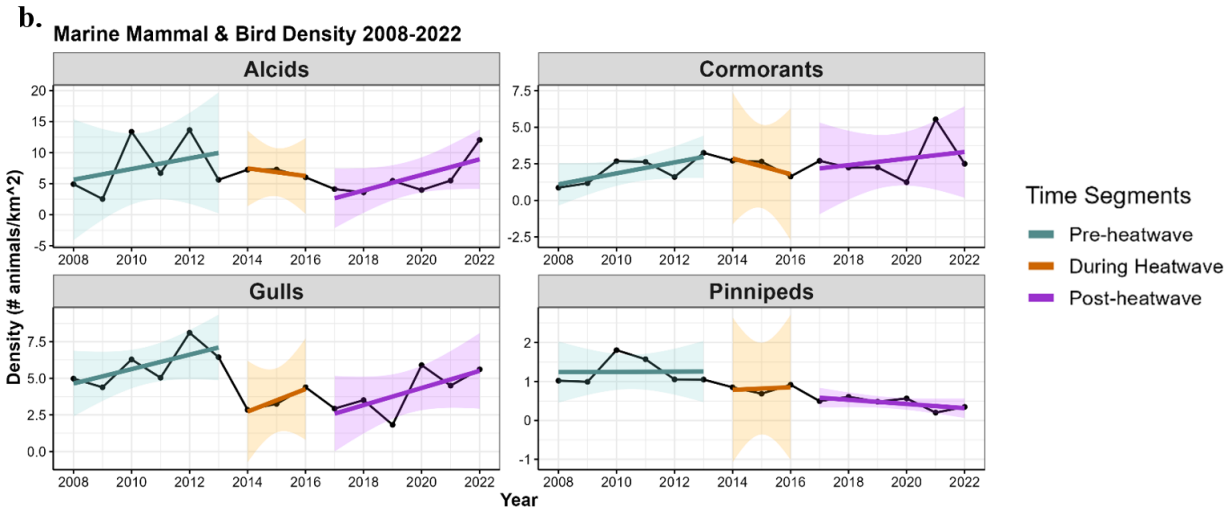

Figure 8. Depicted above is the observed abundance of marine mammal and bird groups that were of focus for this study. The x-axis represents year while the y-axis represents density of animals. The plots are broken apart by study species, with annual averages represented by the black line. For Figure 8A, linear regression lines are represented in blue to identify general patterns of annual density throughout our time series. For Figure 8B, the colored lines designated under the "Time Segments" legend indicate the trend of density through the different heat regimes.

3.b. Correlation between groups

A correlation test between all variables, both environmental and biological was conducted to assess the inherent correlation between all components of the factors going into the MAR model (Figure 9). In total, seven groups were found to have significant correlations including SST & PAR, Fish Abundance & Alcids, Gulls & Alcids, SST & Gulls, PAR & Fish Condition, PAR & Gulls, and Year & Pinnipeds. A table of results is depicted below of correlation values and respective groups (*Table 6*).

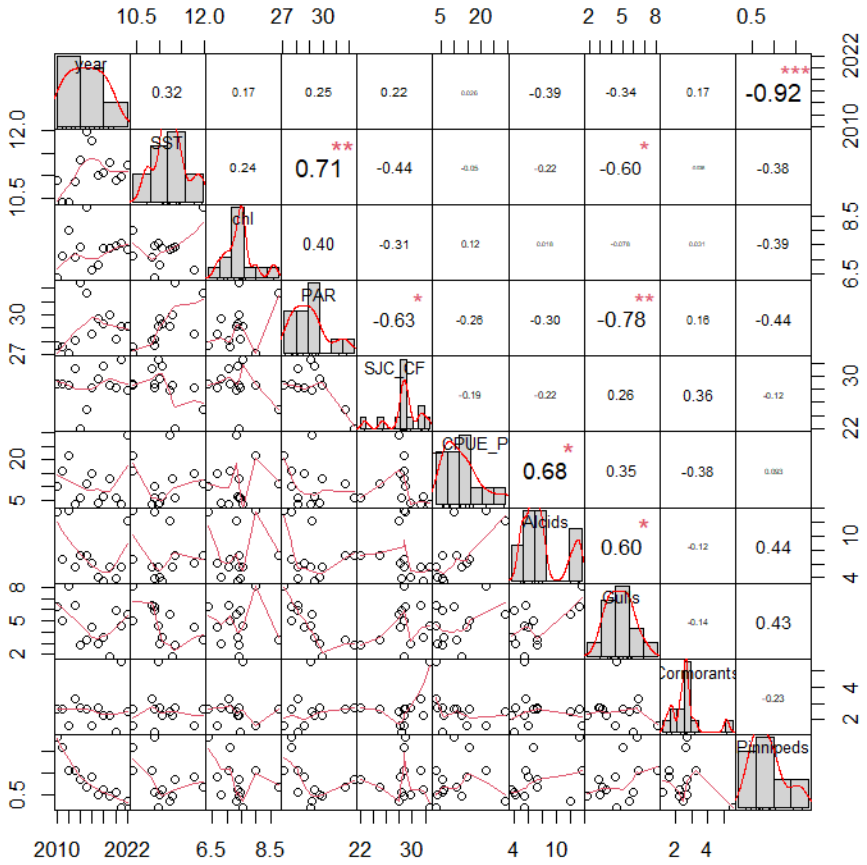

Figure 9. Depicted above is a correlation plot of all the variables involved in this study. The components included are year, SST (sea surface temperature), chl (chlorophyll), PAR (photosynthetically active radiation), SJC_CF (San Juan Channel Condition Factor), VV_CPUE_PSL (San Juan Channel Fish Abundance), Alcids, Guls, Cormorants, Pinnipeds. The central diagonal row of boxes indicates the spread of the data within each of the groups respectively. The axes for these groups are listed externally of the plot, in line with the row/column that the variable resides in. The linear graphs on the left side of the distribution plots indicate the various variables plotted against one another, while the right side of the distribution plots indicate the correlation and its respective significance based on size of numbers and the presence/absence of an asterisk (*). The larger the number, the greater the correlation. The presence of an asterisk indicates significance.

Table 6. Depicted below are the significant correlations detected by the chart.Correlation function. Under groups are the interaction pairs and under correlation are their respective correlations, listed from most positive to most negative correlations. A negative correlation indicates a negative relationship, while a positive correlation indicates a positive relationship.

Groups	Correlation
SST & PAR	+0.71
Fish Abundance & Alcids	+0.68
Gulls & Alcids	+0.60
SST & Gulls	-0.60
PAR & Fish Condition	-0.63
PAR & Gulls	-0.78
Year & Pinnipeds	-0.92

3.c. MAR model outputs

For the MAR model, SST, PAR and chlorophyll were inputted as environmental covariates (C) while Pacific Sand Lance condition and abundance, alcid, gull, cormorant and pinniped observed abundance were incorporated as the biological variables in the model as mentioned in methods. The biological components were input into a 6x6 matrix, while the environmental covariates were tested against the biological components in a 3x6 matrix. The results of the study are shown below (*Figure 10*). Significant relationships between both the environmental covariates and biological components as well as the biological components with themselves were found across groups. For the biological parameters, 18 of the 30 biological parameter outputs were found to be significant. A table outlining the significant results is outlined below (*Table 7*).

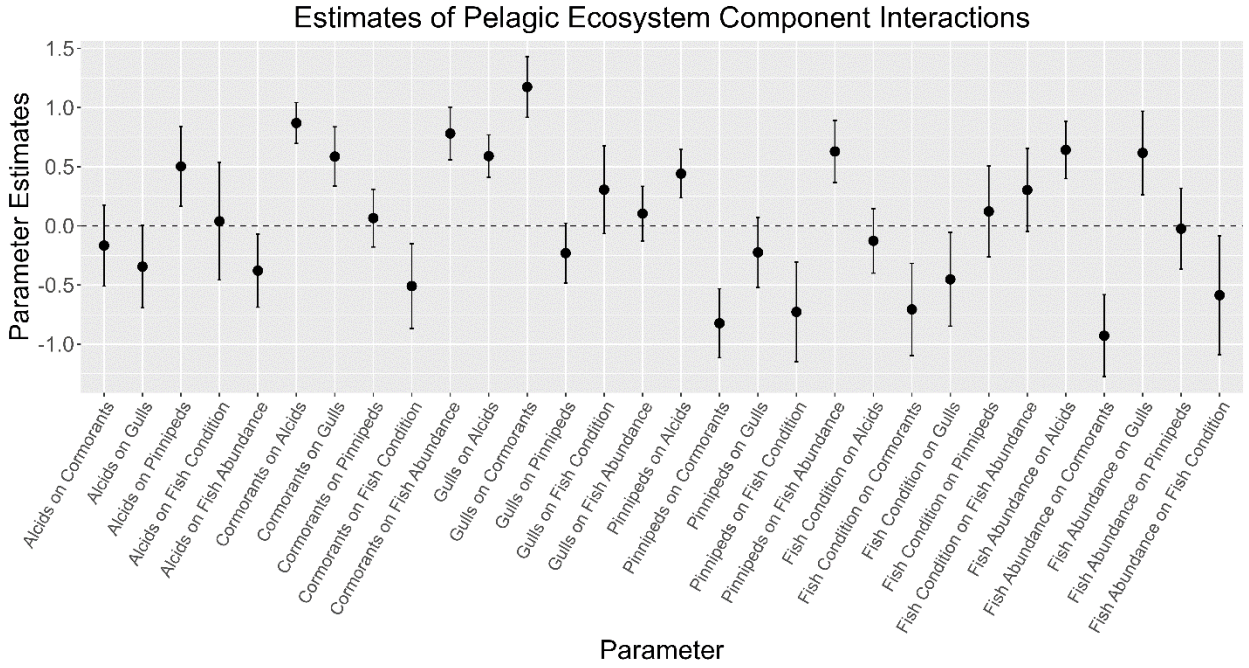

Figure 10. Depicted above are the parameter outputs for the biological matrix within the MAR model. The parameter tested is depicted on the x-axis while the parameter estimate is depicted on the y-axis. Parameter outputs are indicated by a solid circle, while confidence intervals are added in the form of bars around the parameter output. The dashed line crossing the center of the plot indicates a neutral relationship, and any parameter outputs whose confidence intervals cross this

line are deemed insignificant. A positive parameter output indicates a positive relationship between the two biological variables while a negative parameter output indicates a negative relationship between the two biological variables.

Table 7. Depicted below are the significant relationships detected by the MAR model. The left column displays the relationship and is read as "the influence of x on y" while the right column displays the value that the model calculated for the given parameter. A negative parameter output indicates a negative relationship, while a positive parameter output indicates a positive relationship.

Relationship Tested	Parameter Output
Fish Abundance on Cormorants	*-0.92883*
Pinnipeds on Cormorants	*-0.82334*
Pinnipeds on Fish Condition	*-0.72757*
Fish Condition on Cormorants	*-0.70618*
Fish Abundance on Fish Condition	*-0.58620*
Cormorants on Fish Condition	*-0.50920*
Fish Condition on Gulls	*-0.45227*
Alcids on Fish Abundance	*-0.37881*
Pinnipeds on Alcids	*+0.44128*
Alcids on Pinnipeds	*+0.50281*
Cormorants on Gulls	*+0.58599*
Gulls on Alcids	*+0.58969*
Fish Abundance on Gulls	*+0.61675*
Pinnipeds on Fish Abundance	*+0.62890*
Fish Abundance on Alcids	*+0.64188*
Cormorants on Fish Abundance	*+0.78086*
Cormorants on Alcids	*+0.86928*
Gulls on Cormorants	*+1.17392*

For the environmental covariates, and more specifically sea surface temperature, the model indicated that two of the six biological variables were significantly influenced by sea surface temperature (*Figure 11A*). For photosynthetically active radiation, it was found that there was a significant influence on four of the six biological components (*Figure 11B*). For chlorophyll, the model found that three of the six biological components were significantly

influenced by chlorophyll (*Figure 11C*). A table outlining these results is showcased below (*Table 8*).

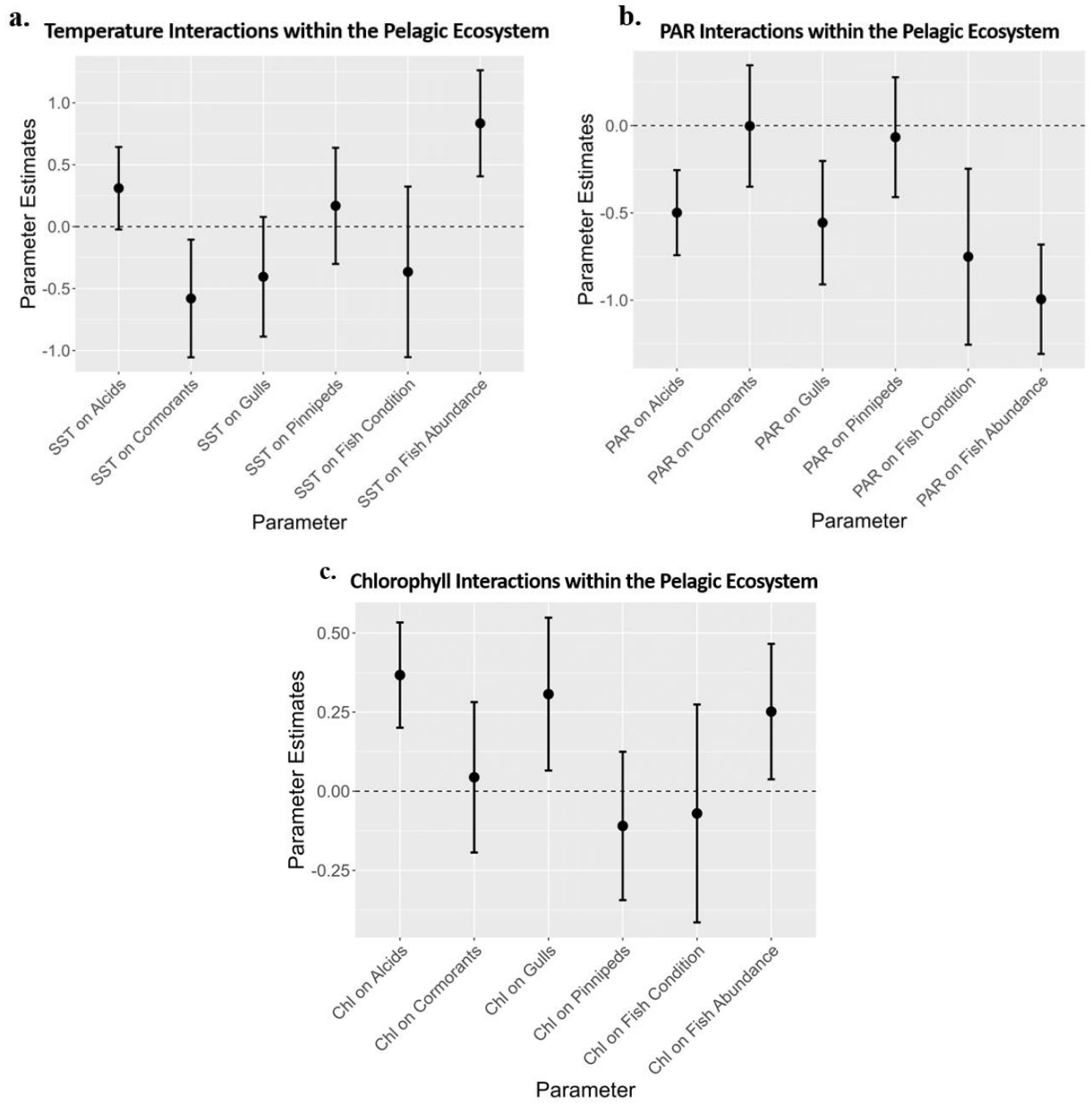

Figure 11. Depicted above are the parameter outputs generated by the MAR model when biological parameters were compared with environmental covariates and their respective parameter outputs, which relationships are depicted on the x-axis. The y-axis represents the parameter estimate, with the points within the graph depicting the parameter outputs generated by the MAR model, with confidence intervals added to these estimates. The dashed line crossing the center of the plot indicates a neutral relationship, and any parameter outputs whose confidence intervals cross this line are deemed insignificant. A positive parameter output indicates a positive relationship between the two biological variables while a negative parameter output indicates a negative relationship between the two biological variables. Figure 11A depicts

the parameter outputs upon the comparison of the biological parameters with the environmental covariate sea surface temperature. Figure 11B depicts the parameter outputs upon the comparison of the biological parameters with the environmental covariate photosynthetically active radiation. Figure 11C depicts the parameter outputs upon the comparison of the biological parameters with the environmental covariate chlorophyll.

Table 8. Depicted below are the parameter outputs generated upon the testing of the biological parameters (first column) against the given environmental co-variates: sea surface temperature (second column), photosynthetically active radiation (third column), and chlorophyll (fourth column). Non-significant findings are depicted with NSF while positive parameter outputs indicate a positive relationship and negative parameter outputs indicate a negative relationship.

	Sea Surface Temperature (°C)	**Photosynthetically Active Radiation (µmol m^-2 s^-1)**	**Chlorophyll (mg/m^3)**
PSL Condition Factor	*NSF*	*-0.75114*	*NSF*
PSL Abundance	*+0.83436*	*-0.99459*	*+0.25157*
Alcids	*NSF*	*-0.49881*	*+0.36691*
Cormorants	*-0.58005*	*NSF*	*NSF*
Gulls	*NSF*	*-0.55619*	*+0.30674*
Pinnipeds	*NSF*	*NSF*	*NSF*

4. Discussion

Within this study, a subset of the pelagic ecosystem was assessed to determine how marine heatwaves have been influencing the system through time. Incorporating three different trophic levels, sea surface temperature, photosynthetically active radiation, chlorophyll, pacific sand lance condition and abundance, pinniped observed density, gull observed density, alcid observed density, and cormorant observed density were used to capture influence on interactions within and between abiotic and biotic groups. The first three components (sea surface temperature, photosynthetically active radiation, chlorophyll) were used as environmental covariates to provide both a biological and physical perspective as to how things within the lowest parts of the food web and external factors were influencing higher trophic groups. The other six groups were used as biological factors to understand how marine heatwaves were not only directly impacting various trophic groups of different life history and feeding strategy, but also interactions between the biological groups. For this to be successfully accomplished a full review of the above groups was performed across the thirteen-year time series (2010-2022) that were available for use. The outcome of this study has therefore provided a glance at both the ecosystem status of the pelagic ecosystem within the San Juan Archipelago as well as an understanding of how the marine heatwave signal propagates through marine systems.

4.a. Ecosystem Resiliency in Relation to Marine Heatwave

Upon the analysis of each component individually, a few conclusions were drawn across the different groups that were tested. Firstly, when breaking down the environmental covariates that were used, we saw that all three groups (SST, PAR, chlorophyll) showed a positive to slightly positive trend through time, with SST indicating the only significant trend. In addition to these general trends, we saw via the shifting baselines analysis that sea surface temperature had remained significantly different than pre-heatwave temperatures after the heatwave had subsided. PAR also seemed to not return to pre-heatwave levels, however the difference was not significant enough to justify a complete baseline shift. Chlorophyll seemed to remain stable throughout the time series, with a peak during the heatwave, which is likely indicative of the more optimal conditions that heatwaves can bring for phytoplankton. In summary, this indicates that marine heatwaves do have a direct impact on physical forcing factors of our ocean systems, as well as basal trophic groups that can result in baseline shifts after the heatwave has passed (Olita et al., 2007, Arteaga & Rousseaux 2023).

The phenomenon relating to SST is particularly interesting when placed in the context of the biological parameters that were assessed. It appears that most all abundances (and condition for pacific sand lance) of the biological parameters decreased drastically at the onset of the heatwave, however a steady recovery was made by nearly all these biological components. To break this down further starting with pacific sand lance, their condition initially plummeted after the onset of the marine heatwave. Within the year however, the condition of pacific sand lance was increasing to the point where at the end of the marine heatwave, condition levels had returned to pre-heatwave levels. This indicates that there was a recovery of the condition throughout the duration of the marine heatwave which has been maintained since. When examining fish abundance, the cyclic behavior of the boom-and-bust cycles of abundance appear to be maintained, while the boom cycles appear to correlate with the onset of heatwaves, as shown in the results section. It is important to note that there was a small regional heatwave in 2019 (PSEMP Marine Waters Workgroup, 2020) which we also see is correlated with an increase in the abundance of pacific sand lance, but for the purposes of this study, the focus of the analysis related to the much larger 2014-2016 heatwave. When examining the marine mammal and bird observed densities, we see similar trends with increased lag times in recovery periods as those that were seen in pacific sand lance. Alcids had a one-year lag time where their observed density fell after the onset of the heatwave, and the decline was maintained for two years post marine heatwave. Their populations then began increasing again, with a slight decrease at a one-year lag time to the 2019 heatwave, but after this, continued to increase. The most recent datapoint within the dataset suggests a return to pre-heatwave observed density levels. For gulls, a decrease in observed density was observed two years prior to the heatwave. Similar to pacific sand lance, their densities began increasing through the heatwave, but then steadily declined after the heatwave subsided. This continued until the 2019 heatwave, at which point their observed abundance rapidly increased to levels similar to those pre-heatwave. Cormorants declined slightly through the heatwave with a similar one-year lag time of decline after the onset of the heatwave. Their observed abundance has since been increasing, with a slight decrease one-year after the 2019 marine heatwave, with a rapid recovery that has put their observed density at greater levels than pe-heatwave years. Pinnipeds present a very different pattern to other

biological components, in that their populations began declining in a non-heatwave year in 2010, and since have continued to steadily decline. Given the extreme linear downwards trend, it is thought that there may be external factors such as increased predation by transient killer whales or dispersal from the area due to increased presence of transient killer whales (Shields et al. 2018).

Based on these assessments a trend of recovery can be seen in most biological groups. This highlights a key finding that marine heatwaves cause short-term, pulse like effects where strong intensity in physical change results in a rapid response by the ecosystem, however, the ecosystem quickly restabilizes, despite these signals (Chandrapavan et al. 2019, Fisher et al. 2020, Ducker et al. 2023). Additionally, given the steady recovery in most all groups despite shifted baseline for sea surface temperature that we saw in this study, conclusions can be drawn that not only is recovery possible, but a feature of adaptability is strongly apparent in our ecosystem. This is very important to highlight given the increase in marine heatwave frequency and intensity that we have been seeing (Oliver et al. 2018). Studying occurrences within our systems as such allow us to better understand expected responses, thus enabling us to better manage our systems and prepare for future impacts of marine heatwaves. In addition, these pulse-like changes in our environment allow us to understand climate change impacts as a whole, as they provide snapshots as to what responses to extreme climate phenomena are like (Holbrook et al. 2020).

To expand on the specific responses seen within our systems, the MAR model allows us to see that there are highly variable effects of increased sea surface temperatures, increased PAR and increases in chlorophyll. When dissecting the responses within parameters tested across sea surface temperature influence, pacific sand lance abundance and cormorant observed density was found to be most significantly influenced. Pacific sand lance abundance was found to be positively influenced, indicating that increased sea surface temperatures increased the abundance of these fish. Although not significant, increased sea surface temperatures were also seen to cause a negative response in pacific sand lance condition, which is a common phenomenon that has been previously studied in other systems (Thompson et al. 2019). This tradeoff between abundance and condition may indicate either an obtaining of carrying capacity given the increased abundance of fish or selection for fish that can maintain a lower condition factor (Boldt et al. 2019; Lorenzen & Enberg 2002). In contrast to pacific sand lance abundance, sea surface temperature was found to have a negative influence on cormorant observed abundance. This may be due to increased competition for food or decreased condition of prey species such as pacific sand lance (Arimitsu et al. 2021), however due to the many ecological steps between processes affected by sea surface temperature and cormorants, this relationship may be falsely displayed in our model. When examining the influence of PAR on the system, we can see that many more components are influenced by this physical factor including all components within the system that were tested excluding cormorants and pinnipeds. All influences were deemed to be negative by the model, indicating that an increase in PAR negatively affects many components of the system. The reasons for this are a bit unclear, given the several steps between sunlight and many of the components tested in the system, however things such as increased competition when a system reaches capacity may be possible explanations (Arimitsu et al. 2021). For chlorophyll, three of the six components were found to be positively influenced by increasing chlorophyl

including pacific sand lance abundance, alcids, and gulls. This makes sense from an ecological perspective, given that increased chlorophyll likely indicates increased productivity, and thus a more productive system in general. In regards to increased instances of marine heatwaves, this means that many variable outcomes could be possible. Given the mixture of negative and positive influences of the various environmental components discussed above, it is likely we will see responses as those outlined in this paper where groups will respond relatively quickly to the onset of the marine heatwave but will rapidly recover as they adapt to the change and the system rebalances itself. Ultimately, this again highlights that ecosystems have incredible resilience and are ultimately able to restabilize themselves despite sudden pulse-like changes in their environment.

It is also important to highlight the correlations apparent between components of the system to understand the path of influence of change presented by the marine heatwave. As noted above, there appear to be seven groups of components that are tightly coupled within the system including SST & PAR, Fish Abundance & Alcids, Gulls & Alcids, SST & Gulls, PAR & Fish Condition, PAR & Gulls, Year & Pinnipeds. This indicates that several of the biological groups are tightly coupled with the physical components of the system, highlighting the coupled responses we see between changes in physical components due to the heatwave and the biological components. Given the correlation between these groups, it is possible that changes within these systems could have more significant consequences for associated groups.

Overall, the importance of the outcomes of this study is the resiliency feature that is highlighted within this ecosystem. This is again extremely important to understand as phenomena such as marine heatwaves increase in frequency and intensity, and also for our understanding of the threshold systems can reach without becoming permanently destabilized. This also supports other studies which have seen similar episodes of resiliency within their systems in response to pulse-like climate effects such as marine heatwaves (Chandrapavan et al. 2019, Fisher et al. 2020, Ducker et al. 2023). This concludes that our systems may be more resilient than previously thought, which could have significant implications for future research in this field.

4.b. Marine Heatwaves in the Context of Modeling Science

Given the resiliency displayed in systems to pulse-like effects such as marine heatwaves, it is extremely important to incorporate this ecological response into our modeling of systems when attempting to understand impacts on ecosystems by climate change as a whole. Firstly, it is important to acknowledge that marine heatwaves manifest themselves very differently than climate change in general. Marine heatwaves have apparent intense pulse-like inputs of change to environmental components that are not sustained for extended periods of time. In contrast, climate change is a much more gradual phenomenon that manifests itself as an accumulation of change to our climate and systems over time (Frölicher & Laufkötter, 2018). We see within our study that marine heatwaves can result in sudden, impermanent changes to a system where recovery is still possible given the short duration of the pulse-like signal by the marine heatwave, which contrasts the gradual change and influence climate change has on systems. The contrast between these two signals therefore highlights the need to address these two phenomena separately when assessing impacts of climate change on ecosystems.

Within the ecosystem science field, models are one tool to understand complex systems by simplifying our natural systems into components that can be assessed on a smaller scale (Robinson 2015). Thus, by the nature of modeling, it is easy to smooth over natural processes that we assume to have similar consequences or outputs but are in fact very different (Grimm 1994). Although climate change and marine heatwaves are very much correlated, this study highlights the need to differentiate between these two phenomena, given the different response that ecosystems can have to these pulse-like inputs of marine heatwaves. Without differentiating between the two, the resiliency component of an ecosystem can potentially be smoothed over, which could result in the drawing of false, or biased conclusions on how our systems will change. Additionally, incorporating marine heatwave signal responses by systems in our models allows us to better capture and incorporate this resiliency component into the management of our ecosystems that we would otherwise be missing. This study therefore provides evidence how differential a system's response can be in relation to short, pulse-like change, and why smoothing over this can eliminate or reduce the resiliency potential we see/factor into our modeling and management of our natural systems.

5. Conclusion

In summary, this study reviews the response of the pelagic ecosystem within the San Juan Archipelago to an intense, two-year long heatwave that influenced the system between years 2014 and 2016. Highlighted within this work is the resiliency strongly apparent within the biological components of our system, despite the change to the physical and bottom trophic components induced by the marine heatwave. In addition to resiliency to change, an interesting phenomenon of return to pre-heatwave abundance levels was featured in several of the biological groups tested, where, despite shifting baselines of physical components of the system, the groups were able to adapt to the changes in a pre-heatwave fashion. This compliment of resiliency and adaptability by a system in response to marine heatwaves drives the conclusion that marine heatwaves must be assessed separately from climate change to understand what short-term changes to the system can cause, as well as to inform us on how systems may respond in the future when conditions as such become more permanent.

References

Arimitsu ML, Piatt JF, Hatch S, et al (2021) Heatwave-induced synchrony within forage fish portfolio disrupts energy flow to top pelagic predators. Global Change Biology 27:1859–1878. https://doi.org/10.1111/gcb.15556

Arteaga LA, Rousseaux CS (2023) Impact of Pacific Ocean heatwaves on phytoplankton community composition. Commun Biol 6:263. https://doi.org/10.1038/s42003-023-04645-0

Bagenal TB, Ricker WE (1978) Methods for assessment of fish production in fresh waters. Blackwell Scientific, Hoboken, NJ

Boldt J, Thompson M, Rooper C, et al (2019) Bottom-up and top-down control of small pelagic forage fish: factors affecting age-0 herring in the Strait of Georgia, British Columbia. Mar Ecol Prog Ser 617–618:53–66. https://doi.org/10.3354/meps12485

Cailliet GM, Love MS, Ebeling AW (1986) Fishes: a field and laboratory manual on their structure, identification, and natural history Belmont, CA: Wadsworth Publishing Company. 194 p.

Chandrapavan A, Caputi N, Kangas MI (2019) The Decline and Recovery of a Crab Population From an Extreme Marine Heatwave and a Changing Climate. Front Mar Sci 6:510. https://doi.org/10.3389/fmars.2019.00510

D'Alpaos A (2011) The mutual influence of biotic and abiotic components on the long-term ecomorphodynamic evolution of salt-marsh ecosystems. Geomorphology 126:269–278. https://doi.org/10.1016/j.geomorph.2010.04.027

Ducker J, Joyce PWS, Falkenberg LJ (2023) Mussels show capacity for persistence under, and recovery from, marine heatwaves. Mar Biol 170:120. https://doi.org/10.1007/s00227-023-04274-5

Fisher J, Kimmel D, Ross T, et al (2020) Copepod responses to, and recovery from, the recent marine heatwave in the Northeast Pacific. PICES Press Vol. 28, No. 1

Frölicher TL, Fischer EM, Gruber N (2018) Marine heatwaves under global warming. Nature 560:360–364. https://doi.org/10.1038/s41586-018-0383-9

Frölicher TL, Laufkötter C (2018) Emerging risks from marine heat waves. Nat Commun 9:650. https://doi.org/10.1038/s41467-018-03163-6

Greene HG, Baker M, Aschoff J (2020) A dynamic bedforms habitat for the forage fish Pacific sand lance, San Juan Islands, WA, United States. In: Seafloor Geomorphology as Benthic Habitat. Elsevier, pp 267–279

Grimm V (1994) Mathematical models and understanding in ecology. Ecological Modelling 75–76:641–651. https://doi.org/10.1016/0304-3800(94)90056-6

Hampton SE, Holmes EE, Scheef LP, et al (2013) Quantifying effects of abiotic and biotic drivers on community dynamics with multivariate autoregressive (MAR) models. Ecology 94:2663–2669. https://doi.org/10.1890/13-0996.1

Holbrook NJ, Sen Gupta A, Oliver ECJ, et al (2020) Keeping pace with marine heatwaves. Nat Rev Earth Environ 1:482–493. https://doi.org/10.1038/s43017-020-0068-4

Khangaonkar T, Nugraha A, Yun SK, et al (2021) Propagation of the 2014–2016 Northeast Pacific Marine Heatwave Through the Salish Sea. Front Mar Sci 8:787604. https://doi.org/10.3389/fmars.2021.787604

Lorenzen K, Enberg K (2002) Density-dependent growth as a key mechanism in the regulation of fish populations: evidence from among-population comparisons. Proc R Soc Lond B 269:49–54. https://doi.org/10.1098/rspb.2001.1853

Mac Nally R, Thomson JR, Kimmerer WJ, et al (2010) Analysis of pelagic species decline in the upper San Francisco Estuary using multivariate autoregressive modeling (MAR). Ecological Applications 20:1417–1430. https://doi.org/10.1890/09-1724.1

Mundy PR, Allen DM, Boldt JL, et al (2010) Status and trends of the Alaska Current region, 2003–2008. In: McKinnell SM, Dagg MJ, editors. Marine ecosystems of the North Pacific Ocean, 2003–2008. p 142– 195.

Olita A, Sorgente R, Natale S, et al (2007) Effects of the 2003 European heatwave on the Central Mediterranean Sea: surface fluxes and the dynamical response. Ocean Sci 3:273–289. https://doi.org/10.5194/os-3-273-2007

Oliver ECJ, Donat MG, Burrows MT, et al (2018) Longer and more frequent marine heatwaves over the past century. Nat Commun 9:1324. https://doi.org/10.1038/s41467-018-03732-9

PSEMP Marine Waters Workgroup, Apple J, Wold R, Stark K, Bos J, Williams P, Hamel N, Yang S, Selleck J, Moore SK, Rice J, Kantor S, Krembs C, Hannach G, Newton J (2020) Puget Sound marine waters: 2019 overview.

Robinson S (2010) Conceptual Modelling: Who Needs It?

Royer TC (1998) Coastal processes in the northern North Pacific. In: Robinson AR, Brink KH, editors. The sea. New York, NY: John Wiley and Sons. p 395–414.

Russell BD, Harley CDG, Wernberg T, et al (2012) Predicting ecosystem shifts requires new approaches that integrate the effects of climate change across entire systems. Biol Lett 8:164–166. https://doi.org/10.1098/rsbl.2011.0779

Shields MW, Hysong-Shimazu S, Shields JC, Woodruff J (2018) Increased presence of mammal-eating killer whales in the Salish Sea with implications for predator-prey dynamics. PeerJ 6:e6062. https://doi.org/10.7717/peerj.6062

Thompson SA, García-Reyes M, Sydeman WJ, et al (2019) Effects of ocean climate on the length and condition of forage fish in the Gulf of Alaska. Fisheries Oceanography 28:658–671. https://doi.org/10.1111/fog.12443

Zamon J (2003) Mixed species aggregations feeding upon herring and sandlance schools in a nearshore archipelago depend on flooding tidal currents. Mar Ecol Prog Ser 261:243–255. https://doi.org/10.3354/meps261243

Zuur AF, Fryer RJ, Jolliffe IT, et al (2003) Estimating common trends in multivariate time series using dynamic factor analysis. Environmetrics 14:665–685. https://doi.org/10.1002/env.611